Resonant Guided Wave Networks

Eyal Feigenbaum* and Harry A. Atwater

Applied Physics, California Institute of Technology, Pasadena, California 91125, USA

(Received 8 November 2009; revised manuscript received 5 March 2010; published 7 April 2010)

A resonant guided wave network is an optical materials design consisting of power-splitting elements arranged at the nodes of a waveguide network. The resulting wave dispersion depends on the network layout due to localized resonances at several length scales in the network. These structures exhibit both localized resonances with a $Q \sim 80$ at 1550 nm wavelength as well as photonic bands and band gaps in large periodic networks at infrared wavelengths.

DOI: 10.1103/PhysRevLett.104.147402 PACS numbers: 78.67.Pt, 42.70.Qs, 42.82.Et

In the last two decades, several photonic design approaches have defined new directions for control of optical dispersion. Photonic crystals [1–4] exploit periodic structures to create dispersive Bloch wave modes in materials. Metamaterials [5,6] capitalize on the ''meta-atom'' concept in which superatomic but subwavelength resonant structures enable complex refractive indices not found in nature. In this Letter, we introduce a synthetic approach to optical dispersion control based on resonant guided wave networks (RGWNs) in which power-splitting elements are arranged in two- and three-dimensional waveguide networks. In a typical RGWN, these photonic elements are designed so that power is split equally among the waveguides connected to each element, such that any closed loop of connected waveguides in the network may act as a resonator.

We first demonstrate the RGWN concept with a two-dimensional (2D) network composed of intersecting metal-insulator-metal (MIM) waveguides, illustrated in Fig. 1(a), and study its dispersion dependence on the waveguide properties and the network topology. MIM waveguides support a lowest-order plasmonic mode that does not exhibit modal cutoff in the visible and near infrared wavelength range, allowing for deep subwavelength modal cross sections [7–12]. It was recently reported that a cross junction which consists of two normally intersecting MIM waveguides with subwavelength gap sizes splits the incoming pulse equally four ways [13]. This equal optical power splitting was observed for continuous waves and also for very short pulses of few optical cycles in the near infrared wavelength range, conserving the shape of the input signal. The equal-power split is a result of the subwavelength cross section of the input waveguide that excites the junction with a broad spectrum of plane waves. As such, the equal four-way splitting of optical power is enabled for transmission lines (e.g., MIM and coaxial configurations) but is not easily accessed for purely dielectric waveguides due to their half-wavelength modal cross sections.

A prototypical 2D-RGWN consisting of insulating gaps in a metallic bulk constitutes a network of coupled crossed-waveguide junction elements, which we term as ''X junctions.'' Each X junction element has four waveguide terminals, serving both as inputs and outputs—when an incoming wave enters through one of the ports, it is split evenly between them and is channeled to the four closest neighboring X junction elements by MIM waveguides. This strong coupling to all four neighboring X junctions gives this structure an optical response different from a cross-coupled network of purely dielectric waveguides, where most of the power would be transmitted in the forward direction, with only weak coupling to perpendicular waveguides. In addition, the rectangular metal cladding regions between the insulating waveguides are much thicker than the skin depth, preventing optical power flow through the material except through the waveguide network. This configuration forms a RGWN using relatively simple elements and network topology.

The equal power splitting in an X junction for small gaps was verified numerically and it was also found that the reflected pulse is out of phase (i.e., approximately π-phase shifted) with the sideways and forward transmitted pulses. The power splitting in the Au-air X junction was investigated using the 2D finite-difference time-domain (FDTD) method with a short pulse excitation (26 fs) at a central wavelength of 1.5 μm. The complex permittivity of Au was fitted to tabulated optical data [14]. For these simulations, the gap sizes of the two intersecting MIM waveguides constituting the X junction are equal. As the MIM

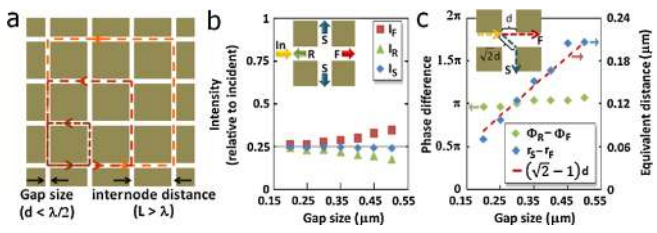

FIG. 1 (color online). (a) 2D RGWN plasmonic implementation and three possible resonant loop trajectories (dashed lines). Power-splitting properties of the emerging pulses in an X junction: (b) intensity and (c) phase difference, relative to the exciting pulse. $\lambda_0 = 1.5$ μm.

gap size is increased above 0.2 μm the optical power flow deviates from equal power splitting between the terminals towards dominant power transmission directly across the X junction [Fig. 1(b)], which resembles the wavelength-scale photonic mode limit [13]. The data of Fig. 1(c) indicates that the transmitted (F) and reflected (R) pulses are out of phase ($\Phi_R - \Phi_F \sim \pi$) and that the phase shift between the sideways-going (S) and the forward transmitted pulses is consistent with the geometrical difference in their pulse propagation trajectories ($r_S - r_F = (\Phi_S - \Phi_F)/k_0 n_{\text{eff}} = (\sqrt{2} - 1)d$).

After characterizing the properties of the RGWN building blocks, we investigate the dynamics of a small network and show that it forms a resonator. A square 2×2 RGWN is composed of four X junctions arranged in a square array, as illustrated in Fig. 2. In order to form a resonance, the network is designed such that when an X junction is excited from the internal ports the exciting waves are out of phase, resulting in constructive interference inside the network, as illustrated in Fig. 2(a). For such out-of-phase excitation the fields in the external terminals interfere destructively, and the power is coupled back into the resonator.

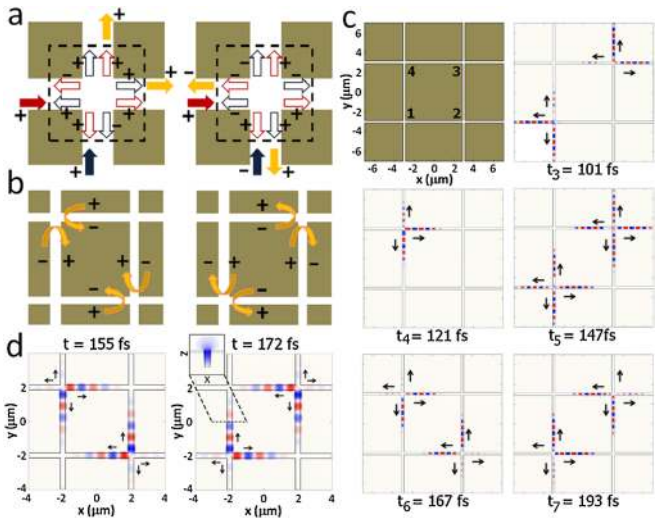

FIG. 2 (color online). Resonance buildup in a 2×2 RGWN. (a) Two out-of-phase input pulses result in constructive interference in the same waveguides from which the pulses entered the junction ($+/-$ correspond to two π-shifted phase states of pulse). (b) Steady states of waves resonating in a 2×2 network where each pair of pulses excites the X junctions out of phase. MIM RGWN: (c) Schematics and snapshots of H_z (normalized to the instantaneous maximal value) at the third to the seventh power-splitting events for a 2D-FDTD simulation. $d = 0.25$ μm, $L = 6$ μm. Channels RGWN: (d) 3D-FDTD of 2D topography of air channel waveguides network; two snapshots of the H field in the parallel plane 0.1 μm underneath the Au-air interface ($z = 0.9$ μm) and an inset showing the H-field distribution in the plane normal to the Au-air interface ($y = 0$). $\lambda_0 = 1.5$ μm and E_x-polarized excitation.

To better understand the interference pattern formation, we develop a simplified analytical description of pulse propagation in the network in which only a few parameters are tracked: phase, amplitude, position, and direction. The pulses are assumed to travel in the waveguides and split into four new pulses upon arrival at an X junction. When the 2×2 RGWN, as shown in Fig. 2(c), is excited from the lower-left arm, the first power-splitting event occurs in junction 1, and the second power-splitting events occur simultaneously in junctions 2 and 4. The third power-splitting event occurs as the pulses arrive at junctions 1 and 3, where each of the junctions is simultaneously excited by two waveguides. The incoming pulses arrive at both junctions in phase, which would result in destructive interference if the R and S split components of each pulse were exactly π-phase shifted. However, the interference is not completely destructive due to the finite size of the waveguides, which causes the phase difference to deviate from a perfect π-phase shift. This power-splitting event determines how much power couples into the network. For all future power-splitting events after the third one, the two pulses arriving simultaneously at each junction are out of phase and therefore interfere constructively inside the resonator. The trade-off between coupling power into the resonator and maintaining it inside suggests that MIM gap sizes that are subwavelength, but not arbitrarily small, will maximize the network resonance.

The model predictions are verified by 2D FDTD simulations with perfectly matched layers at the boundaries, showing that the network dynamics are characterized by an initial propagation transient, followed by the development of a resonant state. Figure 2(c) depicts the simulation snapshots for the first power-splitting events. After the transient that includes the first five splitting events, the resonant state is approached as pairs of pulses resonate between junctions 1 and 3 (exemplified by snapshot t_6) and junctions 2 and 4 (exemplified by snapshot t_7). Similar to the analytical model, we find that in the third power-splitting event, the two pairs of pulses excite the junctions almost in phase, and so only a small fraction of the initial power is coupled into the 2×2 network. During the fourth and fifth splitting events, there is a strong asymmetry in pulse transmission between the two exciting pulses arriving at each junction, as the power reflected back towards junction 2 is negligible with respect to that reflected towards junction 4.

For the same 2D network topology, but with 3D high aspect ratio Au-air channel plasmon waveguides [15], the observed wave dynamics closely resemble that of the 2D MIM waveguide network. The 2×2 2D network of channel plasmon waveguides, consisting of rectangular air-core channels in an Au film, was studied with 3D full-field simulations [Fig. 2(d)]. If the aspect ratio of the channel plasmon waveguide is high enough, the propagating mode within the channels strongly resembles the MIM gap plasmonic mode [15,16]. This can, for instance, be seen in the measured quality factors of RGWNs composed of channel

plasmon waveguides (3D simulations) and MIM slot waveguides (2D simulations) which have Q factor values of 82 and 83, respectively, at a wavelength of 1.5 μm (calculated from the decay rate of the fields after a pulse excitation). Furthermore, the two power-splitting events that define the RGWN resonant state [Fig. 2(b)] are similar for both the channel [Fig. 2(d)] and MIM waveguides [Fig. 2(c)].

The Q factor values of the RGWN in Fig. 3(a) illustrate the role of interference in generating strong network resonances, which cause the network Q factor to be an order of magnitude larger than what would be expected if optical power splitting in the X junctions operated incoherently, i.e., lost half the power in each splitting event. Increasing the MIM gap size causes the phase of the interfering waves to deviate from being π-phase shifted, which results in a degradation in the constructive interference inside the resonator and a decrease in the network Q factor. On the other hand, as the gap size is decreased, the plasmonic mode attenuation increases due to metallic waveguide losses. Between these two competing effects, the maximal Q factor value is obtained for a gap size of 250 nm. These RGWN Q factor values are comparable to typical values of dielectric resonators with similar dimensions that are dominated by radiation loss, e.g., $Q \sim 100$ for the case of a cylindrical dielectric cavity of radius $= 1.3\lambda$ and purely real refractive index of $n = 2.5$ surrounded with air [17]. If we were to artificially decrease the Au loss at 1.5 μm (or alternatively go to higher wavelengths), the Q factor of the resonator would increase tremendously (e.g., $Q = 750$ for a 200 nm gap width), indicating that the resonator Q factor is primarily limited by the material loss.

RGWNs have features that are also broadly reminiscent of Mach-Zehnder interferometers. Figure 3(b) plots the effect on the Q factor of introducing a 1 μm long dielectric region into one of the waveguide gaps. It indicates that while the RGWN may be sensitive to dielectric gap defects and inhomogeneities, the Q factor does not drop abruptly to zero, exemplifying the network robustness to fabrication imperfections.

After studying the resonance effects in small 2×2 RGWNs, we further investigated the dispersion characteristics of infinite 2D periodic RGWNs using FDTD simulations of the structure unit cell surrounded by Bloch boundary conditions. We find that RGWNs exhibit wave dispersion and photonic band gaps due to interference effects, and that the band structure can be controlled by modifying the network structural parameters. Two different length scales control the network dispersion: the subwavelength width of the MIM gaps determines the phase shift at each X junction, and the wavelength-order distance between the nodes along with network topology determine the interference scheme. If the network parameters are chosen such that plane-wave excitation at a given incidence angle results in a resonance effect similar to the one demonstrated for the 2×2 network, then this would correspond to a forbidden state of propagation on the photonic band diagram. Examining the optical density of states (DOS) for different wave vectors over frequencies in the near infrared range, where the material dispersion is small, we observe a photonic band structure which is only due to dispersion resulting from the network topology, as shown in Fig. 4(a). The k vectors for the DOS are extracted from the frequency spectrum of multiple monitors recording the fields of multiple broadband dipoles exciting the structure. The functionality of the infinitely large RGWN is not hindered by loss since its dispersion depends on the waveguide decay length being much larger than the largest resonant feedback loop size that has dominant contribution to the RGWN dispersion. As illustrated in Fig. 4(b), the photonic band structure is scalable with the internode distance since it is what determines the wave retardation between junctions. The MIM gap size does not exhibit the same dependence; instead the band wavelength varies inversely with MIM waveguide gap size. Further possibilities for achieving band dispersion control are illustrated in Fig. 4(c), where we observe the appearance of flat bands

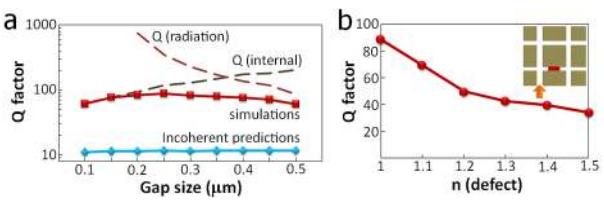

FIG. 3 (color online). Q factors of Au/air MIM 2×2 RGWN resonator. (a) Q factors from simulation results compared with those resulting from incoherent power splitting. The Q factor contribution of the material loss is calculated from the attenuation coefficient [17]. (b) Q factor vs the refractive index of a 1 μm long defect. $d = 0.25$, $L = 4$ μm, $\lambda_0 = 1.5$ μm.

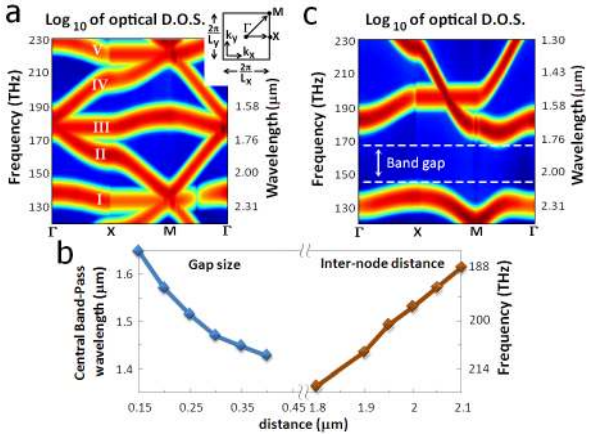

FIG. 4 (color online). Photonic band structure of an infinitely large periodic RGWN. (a) Optical DOS for a square periodic unit cell with $d = 0.25$ μm, $L = 3$ μm. (b) Dependence of photonic band III [at Γ point at $\sim$180 THz in (a)] on L for $d = 0.3$ μm, and on d for $L = 4$ μm. (c) Photonic band gap formed in the optical DOS in rectangular periodic unit cell. In the x direction: $d = 0.24$ μm, $L = 2$ μm; in the y direction: $d = 0.2$ μm, $L = 1.2$ μm.

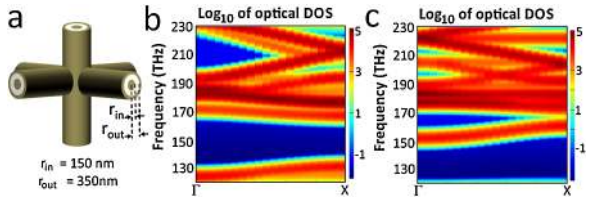

FIG. 5 (color online). 3D RGWN: (a) rendering of a 3D RGWN building block (6-arm junction). Optical DOS of an infinite 3D network spaced periodically with cubic periodic unit cell (b) $L = 2$ μm and (c) $L = 2.2$ μm.

over a wide range of wave vectors at 130 and 170 THz, as well as the formation of a photonic band gap between 140–160 THz, for appropriately chosen network parameters.

The dispersion design in a volume can be addressed by 3D-RGWN topologies, for example, constructing an array of orthogonally intersecting 3D networks of coaxial Au-air waveguides aligned in a Cartesian grid [Fig. 5(a)]. In this case, the four-arm X junction element of the 2D network is replaced by a six-arm 3D junction element. Using 3D FDTD, we have verified that six-way equal power splitting occurs for pulsed excitation in a coaxial Au-air waveguide junction. Like for the 2D-RGWN, the dispersion of the infinitely large periodic 3D-RGWN is predominantly determined by the network parameters rather than the waveguide dispersion. This is demonstrated by the noticeable difference in the band diagrams [Figs. 5(b) and 5(c)] obtained for two networks composed of the same waveguides but with different internode distances.

RGWNs is a different approach for designing dispersive photonic materials. They are distinctly different from photonic crystals, which rely on the formation of Bloch wave states by interference of waves diffracted from an array of periodic elements, which is truly a nonlocal phenomenon. By contrast, RGWNs coherently superpose power flowing along isolated waveguides at X junctions. Furthermore, in a photonic crystal, the interference pattern of the diffracted waves depends on the *nonlocal* periodic spatial arrangement of the diffracting elements, whereas in RGWNs it is the *local* network topology that determines the dispersion and resonance features. For example, in the RGWN, the coherent wave propagation through the network is determined only by the total path length along the waveguide and the phase shift upon power splitting, having no restriction on whether the waveguides are straight or curved. Metamaterials also feature a design approach based on the attributes of localized resonances, but their dispersive properties do not depend on any length scale between resonant elements—thus differing substantially from RGWNs. Arrays of coupled resonator optical waveguides (CROWs) feature discrete identifiable resonators that act as the energy storage elements, and dispersion occurs as modes of adjacent resonators are evanescently coupled [18]. By contrast, in RGWNs, energy is not stored resonantly in discrete resonators, but rather in the network of waveguides that are designed to exhibit a collective resonant behavior. While previously reported resonant plasmonics circuits (e.g., [19–22]) have fundamentally one-dimensional topologies (input-device-output), RGWNs are fundamentally different being 2D and 3D constructs that mediate and regulate power flow in a *material* rather than in a discrete device. While simple examples have been illustrated here, we note that in the most general case of a RGWN, the dispersion-controlling parameters, e.g., the power-splitting elements and waveguide lengths, need not be homogenous or isotropic across the network.

We wish to acknowledge S. Burgos for valuable discussions, and support from the Office of Basic Energy Sciences under Contract No. DE-FG02-07ER46405. E. F. acknowledges financial support from the Rothschild Foundation.

*eyalf@caltech.edu

[1] E. Yablonovitch, Sci. Am. **285**, 46 (2001).
[2] J. D. Joannopoulos *et al.*, *Photonic Crystals: Molding the Flow of Light* (Princeton, New Jersey, 2008), 2nd ed.
[3] A. R. McGurn and A. A. Maradudin, Phys. Rev. B **48**, 17 576 (1993).
[4] G. Shvets and Ya. A. Urzhumov, J. Opt. A **7**, S23 (2005).
[5] D. R. Smith, J. B. Pendry, and M. C. K. Wiltshire, Science **305**, 788 (2004).
[6] V. M. Shalaev, Nat. Photon. **1**, 41 (2007).
[7] W. L. Barnes *et al.*, Nature (London) **424**, 824 (2003).
[8] E. N. Economou, Phys. Rev. **182**, 539 (1969).
[9] B. Prade, J. Y. Vinet, and A. Mysyrowicz, Phys. Rev. B **44**, 13 556 (1991).
[10] R. Zia *et al.*, J. Opt. Soc. Am. A **21**, 2442 (2004).
[11] J. A. Dionne *et al.*, Nano Lett. **6**, 1928 (2006).
[12] E. Feigenbaum and M. Orenstein, J. Lightwave Technol. **25**, 2547 (2007).
[13] E. Feigenbaum and M. Orenstein, Opt. Express **15**, 17948 (2007).
[14] E. D. Palik, *Handbook of Optical Constants of Solids* (Academic, San Diego, 1998), 2nd ed.
[15] S. I. Bozhevolnyi *et al.*, Nature (London) **440**, 508 (2006).
[16] E. Moreno *et al.*, Opt. Lett. **31**, 3447 (2006).
[17] J. Heebner *et al.*, *Optical Microresonators: Theory, Fabrication, and Applications* (Springer, London, 2008).
[18] A. Yariv *et al.*, Opt. Lett. **24**, 711 (1999).
[19] Y. Matsuzaki *et al.*, Opt. Express **16**, 16314 (2008).
[20] S. G. Lin and X. Huang, Opt. Lett. **33**, 2874 (2008).
[21] J. Jung, T. Sondergaard, and S. I. Bozhevolnyi, Phys. Rev. B **79**, 035401 (2009).
[22] A. Hosseini and Y. Massoud, Appl. Phys. Lett. **90**, 181102 (2007).